Available online at www.CivileJournal.org

Civil Engineering Journal

(E-ISSN: 2476-3055; ISSN: 2676-6957)

Vol. 11, No. 10, October, 2025

Enhancing Post-Fire Performance of Lightweight RC Slabs Using Expanded Polystyrene and Steel Fibers: An Experimental Study

Alaa A. Abd [1*], Rafaa M. Abbas [1]

[1] *Department of Civil Engineering, College of Engineering, University of Baghdad, Baghdad, Iraq.*

Received 10 May 2025; Revised 23 August 2025; Accepted 03 September 2025; Published 01 October 2025

Abstract

Aggregate significantly influences the mechanical properties of concrete material and has a crucial role in post-fire behavior. This research focuses on investigating the post-fire behavior of a fiber-reinforced one-way slab made from lightweight expanded polystyrene (EPS) aggregate concrete. The experimental study consisted of testing fourteen fiber-reinforced self-compacting concrete (SCC) one-way slabs with EPS as a partial replacement of coarse aggregate. All specimens have identical dimensions of 1800×500×125 mm. The main parameters investigated included fire exposure, EPS replacement ratio, and steel fiber content. The tested specimens were divided into two groups. The first group included seven specimens tested under monotonic static load, whereas the seven specimens of the second group were tested under monotonic static load after being exposed to a steady-state temperature of 700°C for one hour. Following exposure to fire, results revealed a dramatic decrease in the structural performance of the slab specimens, including cracking load, ultimate load, stiffness, absorbed energy, and ductility, especially for the non-fibrous lightweight samples. However, adding EPS beads in the concrete mixture helps in reducing strength degradation due to fire exposure, and the higher the EPS content, the less strength degradation. This result exposed the positive impact of EPS on the structural performance of RC lightweight slabs exposed to fire due to their thermal properties. Moreover, results revealed a significant enhancement in post-fire stiffness, ductility, and absorbed energy of the RC slab due to steel fiber inclusion, showing their constructive impact on the slab performance.

Keywords: Fire Resistance; Lightweight EPS Concrete; One-Way RC Slab; Steel Fiber; SCC; Flexural Behavior.

1. Introduction

In recent decades, the construction of multi-story buildings has increased, resulting in greater dead weight for the structural components. Therefore, it is essential to focus on reducing the dead weight of structures by utilizing lightweight elements [1]. Structural lightweight concrete (LWC), compared to normal weight concrete, provides a vital improvement in terms of technical, economic, and environmental aspects [2-4]. Application of lightweight concrete significantly reduces the cross section of structural elements (i.e., columns, beams, braces, and plates) and, thus, the dead load of the structure and foundation size. Moreover, longer spans, thinner sections, and better cycling load response can be obtained by using lightweight concrete [5]. Generally, lightweight concrete is instrumental in effectively reducing the risk of earthquake damage, as the earthquake acceleration and its magnitude are significantly affected by the weight of a structure. The factors such as lower density, higher strength/weight ratio, lower coefficient of thermal conductivity, better fire resistance, improved durability, and better sound insulation characteristics are considered advantages of lightweight concrete compared with normal concrete. However, parameters related to lightweight particles, such as bulk specific gravity, unit weight, maximum size, particle shape, texture surface, moisture content, and water absorption ratio,

* Corresponding author: alaa.salman2201m@coeng.uobaghdad.edu.iq

http://dx.doi.org/10.28991/CEJ-2025-011-10-03

considerably affect the properties of lightweight concrete [6, 7]. Three common methods are applied to have lightweight concrete: aerated concrete, no-fines concrete [8], and replacement (partially or totally) of natural aggregates with lightweight aggregate or beads [9]. Acetated or cellular concrete is obtained by introducing large air voids within a matrix by chemical admixture, such as foaming agents or aluminium powder (which increases matrix porosity and decreases the unit weight of concrete). No-fines concrete is mostly produced by using a uniform size of coarse aggregate and eliminating the fine aggregate completely from the concrete matrix.

While substituting totally or partially normal-weight aggregate with lightweight aggregate such as pumice [10] and waste rubber [11], expanded polystyrene (EPS) beads is another method to produce lightweight concrete [12]. Though conventional lightweight aggregate is associated with higher water demand and higher absorption value as a result of the porous structure of these materials [13]. In order to eliminate this problem, expanded polystyrene aggregate (EPS) with non-absorbent, hydrophobic, and closed cellular properties [14, 15] was introduced as a lightweight material by Cook [16]. EPS concrete has the potential to be used as structural elements (cladding panels, curtain walls, load-bearing concrete blocks, composite flooring systems, slabs, and T-beams), protective layers (good energy absorption), and insulated concrete [17-19]. Ali et al. [20] showed a comparison between the mechanical characteristics of lightweight and normal-weight aggregate concrete (NWA) reinforced with steel fibers. They found that LWC had better fresh properties but performed poorly in a hardened state compared to NWA. However, Rakaa & Abbas [21] and Abbas & Rakaa [22] showed that structural fiber-reinforced lightweight concrete can be achieved by partially replacing up to 60% of coarse aggregate with EPS beads. Results showed good flexural performance for EPS lightweight reinforced concrete beams when reinforced with steel fibers. EPS is a useful material for reducing concrete weight and improving its workability and insulation. Incorporating expanded polystyrene granules into a concrete mix can create lightweight polystyrene aggregate concrete with varying densities, compressive strengths, flexural strengths, and tensile strengths. Consequently, this approach helps reduce environmental pollution, minimizes valuable landfill space, and promotes sustainability within construction companies [23].

A thorough comparison of drying shrinkage levels among different types of lightweight aggregate concrete (LWAC) revealed that the drying shrinkage strain of EPS concrete is typically not greater than that of other LWAC varieties; however, the density of EPS concrete is generally lower than that of other types of lightweight aggregate concretes [24, 25]. According to literature, EPS is often used as a substitute for aggregates to make concrete lighter and less conductive to heat. EPS consists of discrete air spaces that are scattered through a solid polymer. Lightweight EPS can be bought commercially and used in mortar or concrete to produce light insulating concrete [26]. An advantage of EPS, as seen from an engineering perspective, is that it absorbs less water compared to other LWAs, as it has less room for water in its structure [27]. The fact that EPS thermal conductivity is only 0.03–0.04 W/m.K is a major reason it is chosen for insulation in the construction industry [28]. Mohammed & Aayeel [29] designed and executed an experiment to assess the strength, fracture patterns, and cracks in RC beams made with a mix of recycled EPS replacing some of the coarse aggregate. In the study, 0%, 15%, 20%, 25%, 35%, 45%, or 60% of the needed coarse aggregate was replaced by recycled EPS. Samples showed reductions in tensile splitting strength, compression strength, and modulus of rupture as the EPS content percentage rose. The beam stiffness was improved, while the concrete suffered cracking failure due to the use of recycled expanded polystyrene.

Numerous studies have investigated the effect of fire flame and elevated temperature on LWC behavior. Nemes et al. [30] studied the effect of different types of Lightweight Aggregates (LWA) on the strength and appearance of lightweight aggregate concrete (LWAC) after being heated up to 800°C. They made 8 concrete mixtures with three kinds of LWA and two with normal-weight aggregate concrete. They found that LWAC performed better than NWA concrete up to 500°C but lost more strength at higher temperatures. Dabbaghi et al. [31, 32] found that concrete with lightweight expanded clay aggregate (LECA) has a lower density, better thermal resistance, and slower decline in mechanical properties under high temperatures, making it suitable for fire-resistant structures. Abdel-Jaber et al. [33] investigated the bending characteristics of Reinforced Concrete (RC) beams containing EPS under elevated temperature. Ultimate failure load was determined through experimental tests for all specimens, and the effect of temperatures (300°C and 600°C) on the RC beams containing EPS was also investigated. Results for beams exposed to 300°C demonstrated comparable capacity to the unheated control beams, while at 600°C, a noticeable decline in ultimate load capacity was observed in comparison to the control beams.

Despite having lower compressive strength at ambient temperatures, results demonstrated improved seismic performance when subjected to elevated temperatures compared to normal-weight concrete [34]. The lighter the concrete, the lower the thermal transmittance, which enhances the thermal performance of the slabs under fire conditions. Advanced nonlinear numerical models were created to forecast the thermal and structural behavior of the examined LWC composite slabs concerning temperature and time-displacement [35]. Exposure to temperatures up to 250°C does not significantly affect the mechanical properties of concrete containing Lightweight Expanded Clay Aggregates (LECA), similar to normal-weight concrete. However, as the temperature rises, an increase in the lightweight aggregate content of the mixture leads to improved strength retention following exposure to elevated temperatures [36]. Utilizing a concrete mixture with 84% total aggregate replacement with LECA can result in concrete that exhibits optimal performance in terms of mechanical properties and strength retention under fire conditions, as well as economic and environmental benefits [37]. Abdullah & Mohammed [38] investigated the effect of elevated temperature on LWC containing LECA. They showed that the addition of LECA decreased both the number and width of cracks formed due to fire, as well as mitigated the loss of ultimate load capacity and beam stiffness.

From the presented studies, numerous investigations on different types of lightweight concrete members under fire or elevated temperature are clearly visible in the literature. However, there aren't any studies that explore how the inclusion of steel fiber to strengthen LWC affects the flexural behavior of EPS lightweight concrete slabs subjected to fire exposure. Consequently, the goal of this work is to study how the inclusion of steel fiber reinforcement affects the thermal and structural behavior and strength retention following exposure to fire or elevated temperature of an RC one-way slab made from expanded polystyrene aggregate as a partial replacement of coarse aggregate. Therefore, a carefully prepared experiment program is intended to investigate the contribution of different EPS and steel fiber volume fractions to the structural performance of one-way EPS LWC slab specimens' behavior before and after fire exposure. To cover the objectives of this study, an experimental work involving the casting and testing of 14 fiber-reinforced self-compacting concrete one-way slabs with EPS as a partial replacement of coarse aggregate was designed. Different volume fractions of EPS bead replacement and steel fiber reinforcement were adopted to assess cracking load, ultimate load, stiffness, absorbed energy, and ductility of the tested slab specimens.

2. Experimental Work Details

2.1. Materials

2.1.1. Fine Aggregate

The concrete samples utilized natural sand of a maximum 4.75 mm grain size based on Iraqi Specification (IQS) No. 45/1984 [39] alongside its subsequent releases. Grading for the used fine aggregate is shown in Table 1. Testing results established the sand classification as Zone 3 according to the sieving results.

Table 1. Grading of the fine aggregate

Sieve size (mm)		Cumulative Passing (%)	IQS. No. (45/1984) Limits			
			Zone1	Zone2	Zone3	Zone4
Sieve Analysis	10	100	100	100	100	100
	4.75	97.4	90-100	90-100	90-100	95-100
	2.36	87.2	60-95	75-100	85-100	95-100
	1.18	76.8	30-70	55-90	75-100	90-100
	0.60	65.8	15-34	35-59	60-79	80-100
	0.30	18.6	5-20	8-30	12-40	15-50
	0.15	7.2	0-10	0-10	0-10	0-15
Fineness modulus		2.47	2.3-3.1			
Specific gravity		2.67	Not limited			
Absorption %		1.06	Not limited			
Chemical Test	Sulphate Content SO_3 (%)	0.41	Not more than (0.5) %			

2.1.2. Coarse Aggregate

The concrete mix for every specimen utilized crushed gravel at a maximum size of 14 mm. Test outcome for gravel grading used in this study, shown in Table 2, indicated it matches the limits stated in Iraq Specification (IQS) No. 45/1984 [39] for a gravel maximum size of 14 mm.

Table 2. Test results of the Coarse Aggregate

Sieve size (mm)		Cumulative Passing (%)	IQS. No. (45/1984) Limits		
			40-5 (mm)	20-5 (mm)	14-5 (mm)
Sieve Analysis	75	100	100	-	-
	63	100	-	-	-
	37.5	100	95-100	100	-
	20	100	35-70	95-100	100
	14	98.3	-	-	90-100
	10	84	10-40	30-60	50-85
	5	9	0-5	0-10	0-10
	2.36	1.5	-	-	-
Passing from sieve 0.075		1.5	Max. allowable (3%)		
Specific gravity		2.64	Not limited		
Absorption (%)		0.75	Not limited		
Chemical Test	Sulphate Content SO_3 (%)	0.07	Not more than (0.1) %		

2.1.3. Expanded Polystyrene Beads (EPS)

This investigation used spheres of EPS particles, displayed in Figure 1, to replace coarse aggregate material with a maximum size of 10 mm. Table 3 shows findings for the sieve analysis for the EPS beads grading spectrum that was utilized in this study.

Figure 1. EPS Beads

Table 3. EPS Beads Sieve Analysis

Sieve Size (mm)		Passing %
Sieve Analysis	12.5	100
	9.5	85
	4.75	12.8
	2.36	2.2

2.2. Mix Design

In this research, self-compacting concrete (SCC), designed according to the requirements of EFNARC [40] was adopted as the reference concrete mix. Material constituents used to compose the SCC reference concrete mix included Ordinary Portland Cement (OPC), natural sand, normal-weight coarse aggregate, silica fume, tap water, and Sika's ViscoCrete-180 superplasticizer (SP). The rheological properties for the SCC mixtures used in this study are shown in Table 4. Results presented in Table 4 revealed that all mixtures comply with self-compacting concrete requirements as defined by EFNARC. EPS beads were adopted as a partial replacement of the coarse aggregates to produce the LWC. Different proportions of hooked steel fibers (SF) were used as additional reinforcement. The mechanical properties of the considered steel fibers are illustrated in Table 5**.** Table 6 presents the proportions of the material constituents used to cast each of the fourteen slab specimens employed in the experimental program.

Table 4. Rheological test results of SCC mixtures

Mix designation	EFNARC tests and limits			
	Slump Flow Test	**T50 Test**	**L-Box Test**	**V Funnel Test**
	SF1(550 to 650) SF2(660 to 750) SF3(760 to 850)	VS1(≤ 2) VS2(> 2)	PA1(≥ 0.80 with 2 rebars PA2(≥ 0.80 with 3 rebars	VF1(≤ 8) VF2(9 to 25)
R	730 mm	1.8s	0.889	5s
EPS20SF0	760 mm	1.6s	0.9	6s
EPS20SF0.5	720 mm	2s	0.87	6s
EPS20SF1	680 mm	2s	0.8	7s
EPS40SF0	740 mm	1.5s	0.95	8s
EPS40SF0.5	690 mm	2s	0.82	7s
EPS40SF1	640 mm	2s	0.8	6s

Table 5. Steel fibers' mechanical characteristics

Fiber size, D (mm)	Length, L (mm)	Fiber aspect ratio (L/D)	Yield strength (MPa)
0.5	50	100	1900

Table 6. SCC mixtures composition and proportions for different mix designs

Mix designation	Mix Proportion (kg/m^3)						SP (lit/m^3)	Silica fume* (%)
	Water	Cement	Sand	Gravel	EPS**	SF		
R	185	441	750	950	0	0	4	4
EPS20SF0	185	441	750	760	2	0	4	4
EPS20SF0.5	185	441	750	760	2	39	4	4
EPS20SF1	185	441	750	760	2	78	4	4
EPS40SF0	185	441	750	570	4	0	4	4
EPS40SF0.5	185	441	750	570	4	39	4	4
EPS40SF1	185	441	750	570	4	78	4	4

* Content by weight of cement, ** Replacement by volume of coarse aggregates.

From each concrete mixture indicated in Table 6, two slab specimens have been cast. Moreover, six concrete cubes with dimensions 150×150×150 mm, eight 150×30 mm concrete cylinders, and four prisms 100×100×500 mm have been sampled and cast as control specimens to investigate concrete mechanical properties. Also, an additional one 100×100×100 mm standard cube was prepared to measure concrete thermal properties. Curing for the RC slab specimens and the control concrete specimens (cubes and cylinders) was started 24 hours after concrete pouring. Daily moisturization of these specimens to preserve water content has continued for 28 days. Figure 2 shows slab specimens and the control concrete specimens cast from each concrete mixture.

Figure 2. Casting slab and concrete control specimens

2.3. Tested Specimens

This research involved testing fourteen simply supported fiber reinforced self-compacting concrete (SCC) one-way slab specimens, including two normal weight reinforced concrete slab specimens cast without fiber nor EPS beads used as reference specimens. The tested specimens were arranged into two groups. The first one comprises of seven slab samples tested under monotonic static load at lab ambient temperature, whereas the second group with seven slab samples tested statically after being subjected to fire exposure of (700 ± 10 °C) for one hour. Samples in these groups were arranged into two subgroups in which the first three slab specimens were cast with 20% of the volume of the coarse aggregate replaced with EPS beads to create lightweight concrete (LWC), whereas 40% of the volume of the coarse aggregate were replaced with EPS beads in the second three slab specimens. Moreover, each of the three slab specimens in the subgroups was cast with three different volume fractions of steel fibers (SF); 0%, 0.5%, and 1%. Illustrative flowchart showing the process of the methodology adopted in the experimental program is depicted in Figure 3.

All specimens maintained identical geometrical layouts, with dimensions of 1800 × 500 × 125 mm and a clear span of 1600 mm, as illustrated in Figure 4. Notations for the tested specimens are presented in Table 6. In this notation, the number following EPS refers to the percentage of the volume fraction of coarse aggregate replaced with EPS beads, whereas the number following SF refers to the percentage of volume fraction of steel fiber content in the concrete mixture. The same concrete mixtures presented in Table 6 have been used to cast each of the corresponding seven slab samples in the two groups.

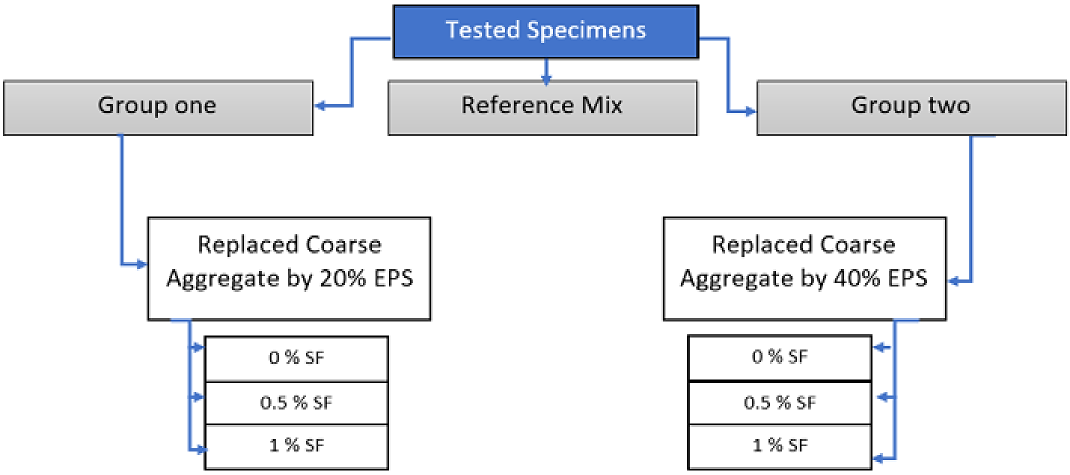

Figure 3. flowchart of the experimental program details

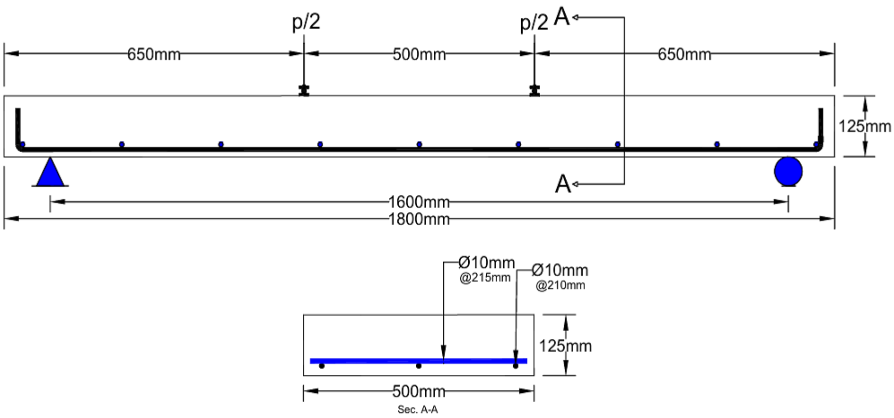

Figure 4. Slab specimen dimensions and reinforcement details

2.4. Furnace and Burning Details

The present study aims to investigate the structural behavior of fire-exposed lightweight concrete slab specimens. To achieve this target, the specimens were placed inside a gas furnace, which has a fire chamber with outer dimensions of 3.50 m in length, 2.00 m in width, and 0.80 m in height, as shown in Figure 5. It is provided with twenty gas burners, eight for each pair of opposing longitudinal sides and two for each transverse side, which are connected to ten gas containers in the sidewalls at the base to provide the heat during the burning test. Two blowers supplied the furnace with air during the fire test to maintain fire intensity and heat distribution. The slab specimens were subjected to burning in a gas furnace, utilizing fire heating under controlled conditions, specifically maintaining a steady-state temperature of 700 ± 10°C for an exposure duration of one hour, as illustrated in Figure 6. A digital thermometer with a K-type sensor wire was employed to monitor and document the temporal variations in temperature in the furnace environment. The temperature-time relationship criteria were established following ASTM E119-14 [41]. After complete fire exposure, the samples were removed from the furnace and allowed to rest at an ambient temperature (30°C) before testing.

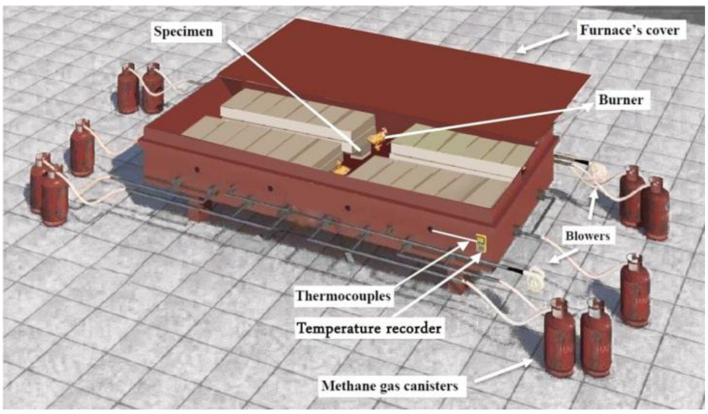

Figure 5. Schematic presentation of the burning furnace

Figure 6. Specimens burning procedure

2.5. Testing Program

To accomplish the aim of this study, samples from the first group have been tested under static load using a test setup shown in Figure 7. However, testing of the fire-exposed slab specimens of the second group was performed in two stages. In the first stage, slab samples have been exposed to fire for a specified time period as indicated in paragraph 2.3. In the second stage, the same slab samples, after being cooled at ambient temperature, were subjected to monotonic static load to determine their residual ultimate load capacity after burning using a test setup shown in Figure 7.

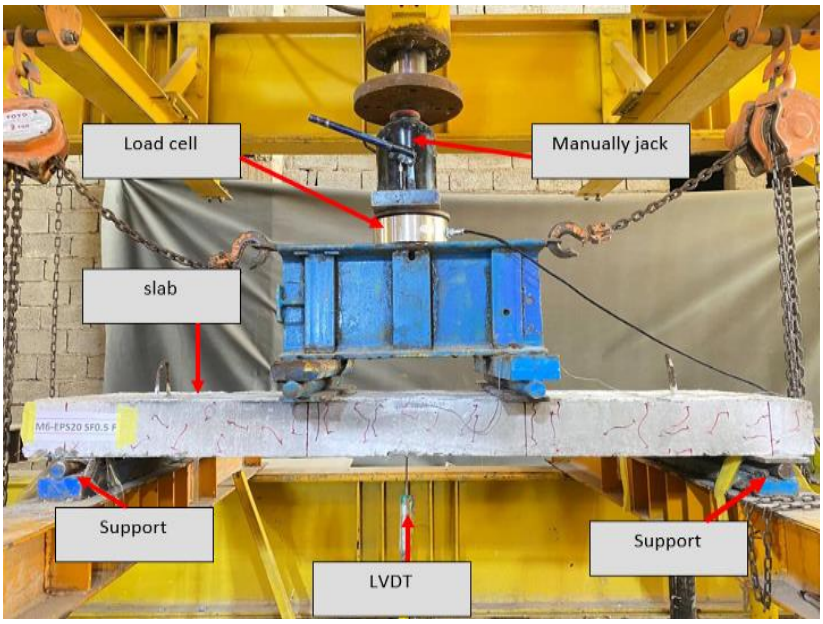

Figure 7. Testing setup

In the static load test program, the slab specimens were supported on two steel supports, allowing for both horizontal and angular movement at one end while permitting only angular movement at the other end, thereby simulating roller and pin supports, respectively. A hydraulic jack applied load to the slab specimens through load cells connected to rigid transverse steel beams, which distributed the load to two points on the top surface of the specimen, simulating a four-point loading testing configuration, as illustrated in Figure 7. Steel rods with a diameter of 30 mm were used to transfer the testing load onto the reinforced concrete slab through steel plates at each point to prevent stress concentrations in the contact area. The two-point loading was applied at the one-third span point of the slab to create a pure flexural region in the middle third of the specimen. Linear Variable Displacement Transducers (LVDTs) were positioned at designated locations and connected to a data acquisition system to capture the setup readings. Subsequently, static loading was applied manually, and the readings from the load cells and LVDTs were recorded by the data acquisition logger, which automatically saved the data to a PC. Deflections at mid-span were measured at each increment of loading.

3. Test Results and Discussion

3.1. Mechanical Properties of Hardened Concrete

Results for the mechanical properties of the hardened concrete are presented in Table 7. In this table, results for concrete cubes compressive strength (f_{cu}), cylinders splitting tensile strength (f_t), and prisms modulus of rupture (f_r) are presented and compared for the control specimens for the burned and unburned samples.

Table 7. Mechanical properties of hardened concrete before and after fire exposure

Mix designation	f_{cu} (MPa)		Residual f_{cu} (%)	f_t (MPa)		Residual f_t (%)	f_r (MPa)		Residual f_r (%)
	Unburned	Burned		Unburned	Burned		Unburned	Burned	
R	57.1	39	68.3	5	3.70	74	6.35	4.80	75.6
EPS20SF0	38.3	31.2	81.5	3.24	2.10	64.8	4.94	3.52	71.25
EPS20SF0.5	41.4	30.20	73	3.85	2.30	59.7	5.73	3.90	68.1
EPS20SF1	43.7	29.30	67	4.98	2.57	51.6	7.95	5.26	66
EPS40SF0	30	21.20	70.7	3	1.90	63.3	4.42	3.16	71.5
EPS40SF0.5	32.3	21.70	67.2	3.28	2.11	64.4	4.95	3.40	68.7
EPS40SF1	37.6	23.20	61.7	3.84	2.26	58.9	7.55	5.03	66.6

Generally, mixtures containing lightweight EPS aggregates exhibited lower mechanical properties at room temperature because of the low strength and density of EPS aggregate, which significantly affects the overall strength of the concrete members made from EPS concrete. However, the presence of steel fiber (SF) significantly enhances concrete mechanical properties, especially flexural and tensile strength, as indicated by previous studies [12, 21]. After burning at a constant temperature at (700°C) a significant reduction in the overall mechanical properties was observed. Reduction in the concrete compressive strength, splitting strength, and modulus of rupture of about 31.7%, 26%, 24.4%, respectively, was recorded for the reference mixture due to fire exposure. Moreover, adding EPS beads to the concrete mixture helps in reducing strength degradation due to fire exposure. Results indicated a reduction of about 18.5%, and 29.3% in the compressive strength when 20% and 40% of EPS beads were added, respectively. However, a greater effect of fire exposure on the tensile properties of the hardened concrete was observed, indicating greater strength degradation due to higher damage to the strength of the concrete matrix and to the adhesion (bond) of the matrix to the aggregate grains. Lightweight aggregates of EPS introduce numerous small voids in concrete, giving them their low density and reducing the weight of concrete, thus low thermal conductivity. These properties indicated that lightweight aggregates of EPS can insulate concrete from heat transfer, prevent cracking and fissuring caused by thermal stress, and better maintain compressive strength and thermal insulation capabilities than conventional aggregates after fire exposure. These findings agree well with other studies [42, 43].

Additionally, results shown in Table 7 revealed that EPS concrete mixture with steel fibers poses greater strength degradation than those without fibers due to fire exposure. For concrete samples with 1% steel fibers, an additional reduction of 14.5% and 9% in the compressive strength, 13.5% and 4.4% in the splitting strength, and 5.2% and 4.9% in the rupture strength was noted for samples with 20% and 40% EPS content, respectively. The steel fiber contributed to deteriorating concrete properties after fire exposure due to its high thermal conductivity. Hence, the higher steel fiber content, the greater strength loss or reduction [20, 25]. Furthermore, these results showed that higher EPS content resulted in less strength degradation due to fire exposure

3.2. Post-Fire Structural Performance

Understanding how concrete behaves at elevated temperatures is very important for understanding materials under extreme conditions. Heating concrete to a high temperature result in its moisture being lost, cracks appearing, and its original strength changing [30]. Observing these modifications helps reveal how concrete holds up under and after exposure to fire.

3.2.1. Burning Cracking

After being exposed to a steady-state temperature of 700 °C for one hour, samples were removed from the furnace and allowed to rest at an ambient temperature. After cooling, specimens have been visually examined for damage and cracks. Generally, cracks appeared on the surfaces, as well as on the sides and bottom, of the slab models due to the fire, as indicated by the cracks marked with red colour shown in Figure 8. The reference sample (R) exhibited a greater crack width compared to the other samples. Notably, the cover of the reference sample had some obvious cracks, as illustrated in Figure 8. However, in spite of samples with EPS content exhibiting a larger number of hair cracks, these cracks were more uniformly distributed with smaller widths as compared to a reference sample. Moreover, the effect of EPS content is more obvious in samples with 40% of EPS content as compared with samples with 20% EPS content. lightweight EPS aggregates samples have lower thermal conductivity and higher fire resistance than regular samples, thus enabling it to withstand higher temperatures and prevent severe cracking or surface damage to the concrete due to fire exposure. Because of the porous nature of lightweight EPS Aggregates, the evaporated water has a place to escape, which reduces the damage occurring within the concrete. On the other hand, samples with higher steel fiber volume fraction, shown in Figure 8, exhibited a lesser number of hair cracks, revealing the effectiveness of steel fibers at controlling temperature cracks due to enhanced concrete tensile strength. The evaluation of the specimen's damage took into account the length of cracks and the spalling area as a percentage of the surface area of the specimen.

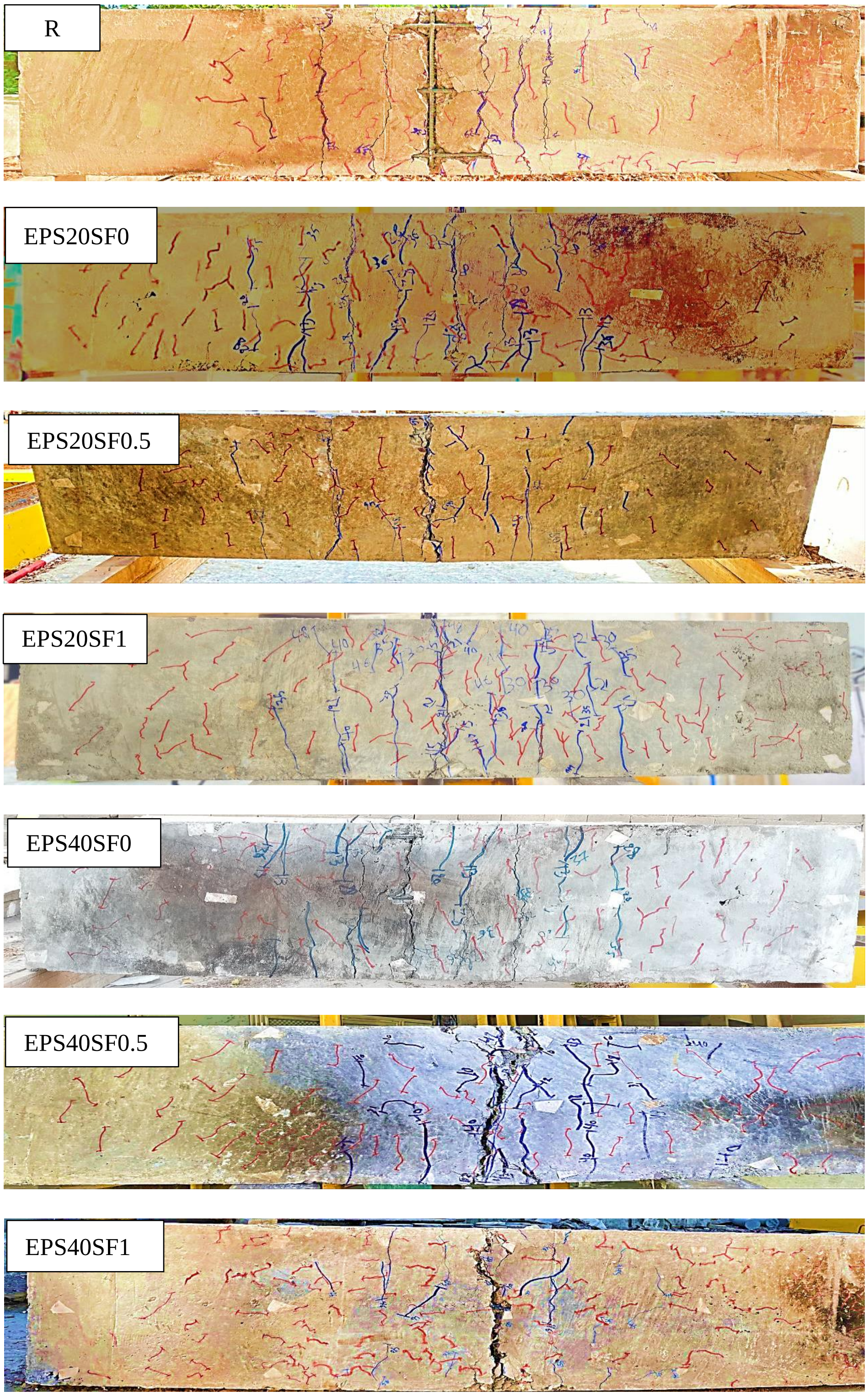

Figure 8. Post-fire and flexural Cracks pattern

3.2.2. Cracking Load, Ultimate Load, and Mode of Failure

After being exposed to elevated temperature and allowed to cool at ambient temperature, slab specimens have been experimentally tested under a four-point loading scheme as shown in Figure 7. Flexural failure was observed in all the burned slabs, with new cracks forming on the sides and bottom of the slabs. The crack patterns due to flexure are highlighted in blue colour cracks as shown in Figure 8. The findings indicated that although the mechanical properties of the unburned control samples diminished after the addition of lightweight EPS aggregates, slabs incorporating EPS beads exhibited greater resilience in their ultimate post-burning load capacity. This suggests that the use of EPS aggregates mitigates the deterioration of the ultimate load-bearing capacity of the burned samples under similar conditions.

Post-fire Results presented in Table 8 and Figure 9 showed that the reduction in the ultimate strength for samples without steel fiber containing 20% and 40% of EPS aggregates was 7.4% and 10.9%, respectively, in comparison to the control sample. However, an obvious increase in the load-carrying capacity was achieved when samples were reinforced with steel fiber. For samples containing 20% and 40% of EPS aggregates and 1% of steel fiber, an increase of 11.4% and 9.2% was recorded, respectively. This can be attributed to added tensile strength of concrete due to steel fiber and to the EPS beads' thermal insulation effect resulted in higher fire resistance relative to a conventional RC slab. Moreover, the comparison presented in Figure 9 indicated that cracking has increased due to steel fiber addition but decreased when the EPS content increased. Finally, the results presented revealed that the first crack appears faster when EPS beads were used and that the first crack is delayed in the presence of steel fibers. Results for the non-fibrous burned samples indicated that a significant reduction of -33.3% and 41.7% in the cracking load due to 20% and 40% of coarse aggregate replacement with EPS beads. However, a considerable enhancement in the cracking load was achieved due fiber reinforcement, which resulted in a maximum reduction of 16.7% in the cracking load when samples reinforced with 0.5% volume fraction of steel fiber. Moreover, results for the burned sample reinforced with 1% fibers, presented in Table 9, showed a maximum enhancement of 50% and 71.4% in the cracking capacity. These results highlighted the superior effect of steel fiber reinforcement that counteracted EPS undesirable impact on the flexural characteristics of the lightweight slab samples.

Table 8. Post-fire cracking and ultimate load variation

Specimens	Cracking load (kN)	Variation (%)	Ultimate load (kN)	Variation (%)
R	12	---	40.3	---
EPS20SF0	8	-33.3	37.3	-7.4
EPS20SF0.5	10	-16.7	43.2	7.2
EPS20SF1	12	0.0	44.9	11.4
EPS40SF0	7	-41.7	35.9	-10.9
EPS40SF0.5	11	-8.3	41.8	3.7
EPS40SF1	12	0.0	44	9.2

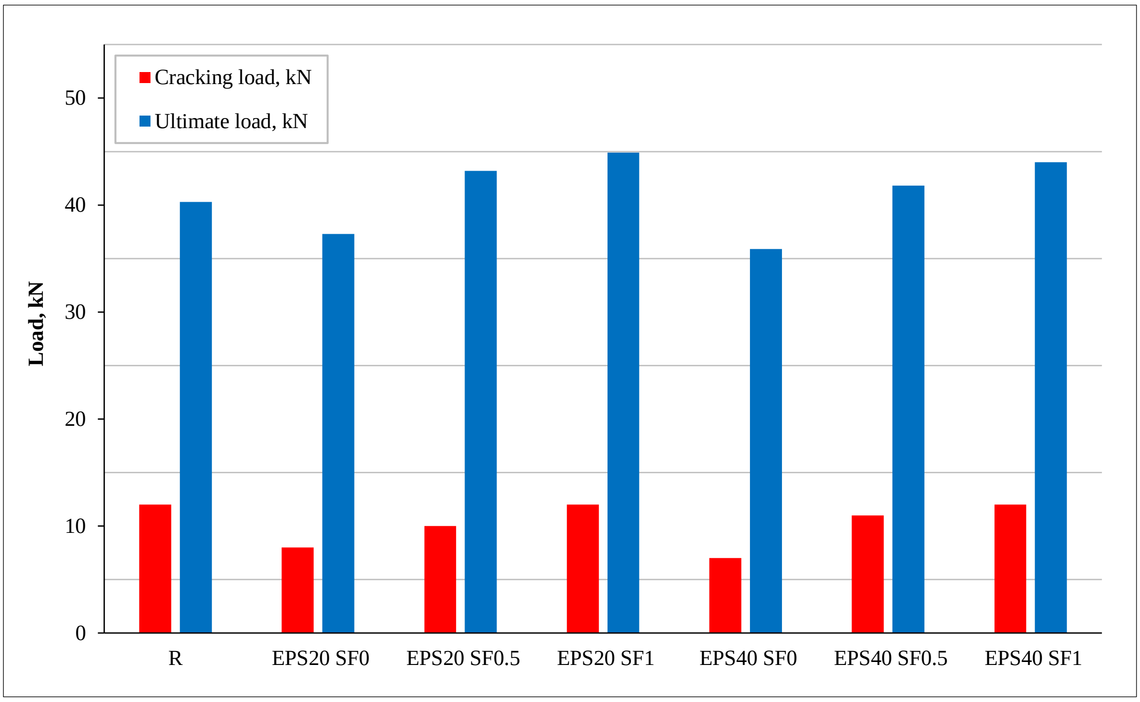

Figure 9. Variation of post-fire cracking and ultimate load

Comparison of post-fire cracking load variation with those for samples that have not been exposed to fire is presented in Table 9 and Figure 10. Comparison presented revealed that the cracking load was significantly reduced due to fire exposure. A reduction ranging from 15% to 33% in cracking load was recorded due to fire exposure for the different ranges of EPS and fiber content in the examined slab samples. However, the results showed that the rate of this reduction was reduced with increasing EPS content due to the EPS beads' thermal insulation effect. On the other hand, increasing steel fiber content inversely affects the rate of cracking load reduction. This result might be attributed to the fact that the steel fiber contributed to deteriorating concrete properties after fire exposure due to its high thermal conductivity, thus the higher impact of fire exposure and a higher rate of strength reduction.

Table 9. Cracking load variation for burned and unburned samples

Specimen	Cracking load (kN)		Variation [1] (%)	Variation [2] (%)	Variation [3] (%)
	Unburned	Burned			
R	15	12	-20.0	---	
EPS20SF0	10	8	-20.0	33.3	---
EPS20SF0.5	13	10	-23.1		25.0
EPS20SF1	16	12	-25.0		50.0
EPS40SF0	8	7	-12.5	41.7	----
EPS40SF0.5	13	11	-15.4		57.1
EPS40SF1	15	12	-20.0		71.4

[1] Burned sample results with unburned ones;

[2] Burned sample results due to EPS content;

[3] Burned sample results due to fiber content.

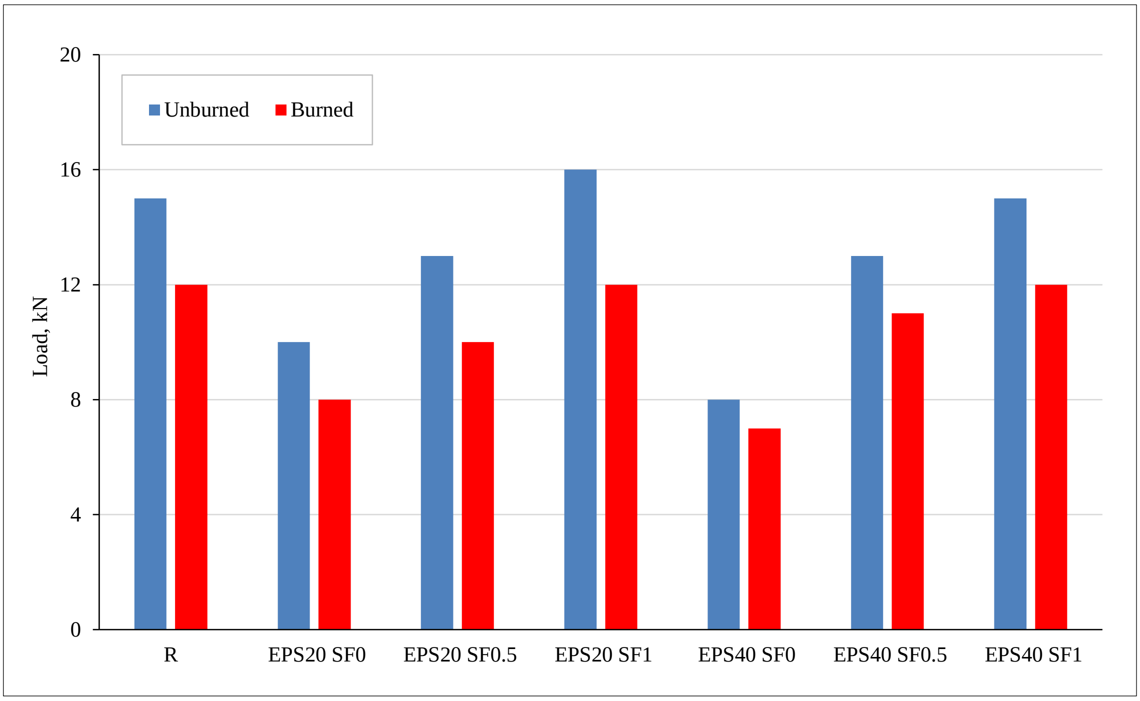

Figure 10. Variation of cracking load for burned and unburned samples

3.2.3. Load-Deflection Behavior

During static load testing of pre- and post-fire specimens, each load increment and vertical deflection of the burned samples were measured at mid-span. The load and deflection behavior of the samples was investigated up to failure. Figure 11 shows the load-deflection behavior of the slab samples after being exposed to fire. The results in this figure are divided into three groups. Group one and group two illustrate the effect of the steel fiber content on the structural response of burned samples with EPS aggregate volume fractions of 20% and 40%, respectively, whereas the third group shows the comparison for the effect of EPS aggregate volume fraction replacement. Ultimate load and deflection variation for the three groups are compiled in Table 10.

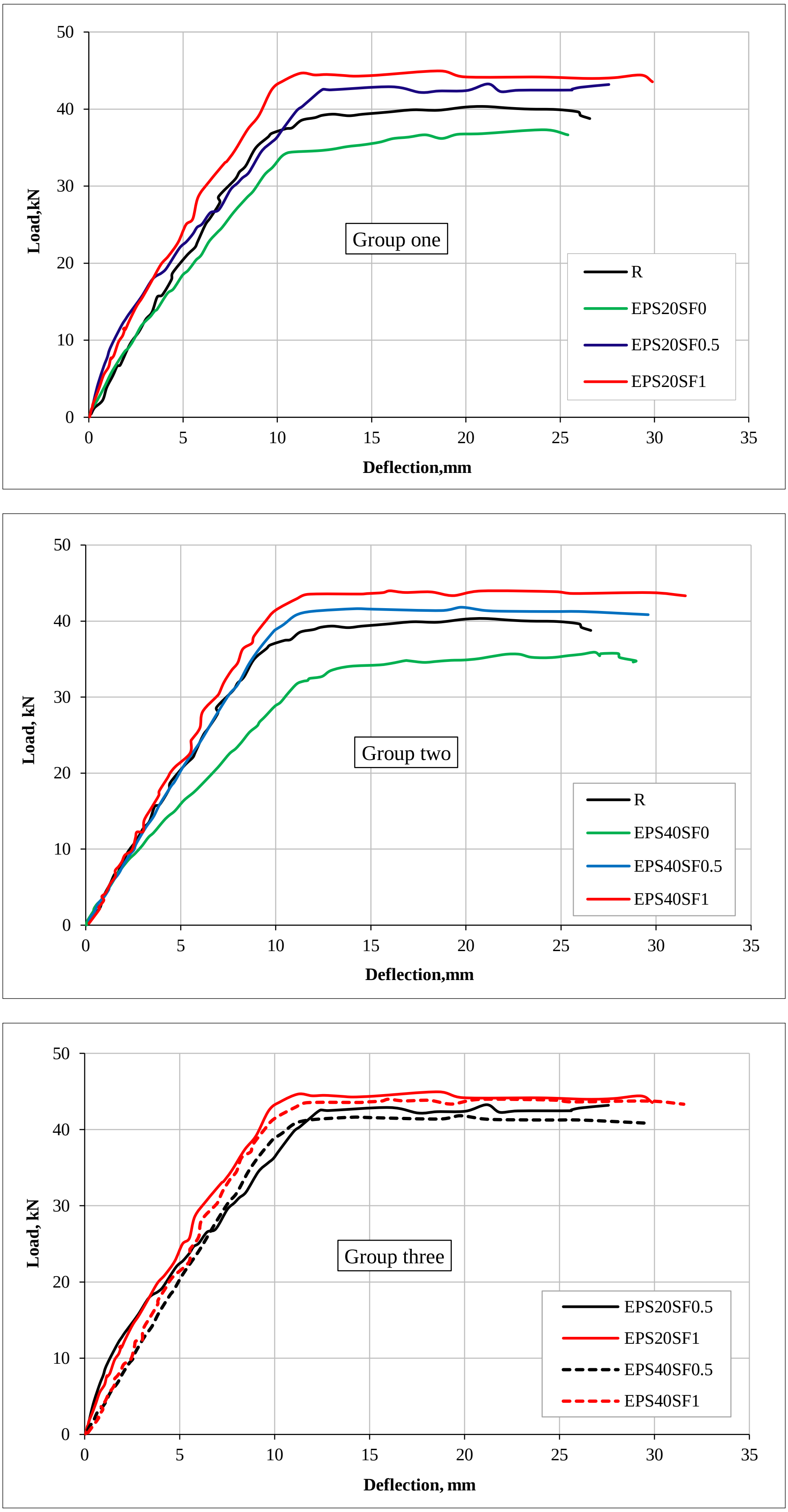

Figure 11. Post-fire load-deflection behaviour

Table 10. Post-fire flexural behaviour of the tested slabs

Specimen	Max. load (kN)	Variation (%)	Δ max. (mm)	Variation (%)
Group one				
R	40.3	----	26.6	----
EPS20SF0	37.3	-7.5	25.4	-4.5
EPS20SF0.5	43.2	7.2	27.5	3.4
EPS20SF1	44.9	11.4	29.8	12
Group two				
R	40.3	----	26.6	----
EPS40SF0	35.9	-11.0	28.7	8
EPS40SF0.5	41.8	3.7	29.6	11
EPS40SF1	44	9.2	31.5	18.4
Group three				
EPS20SF0.5	43.2	----	27.5	----
EPS40SF0.5	41.8	-3.2	29.6	8.7
EPS20SF1	44.9	----	29.8	----
EPS40SF1	44	-2.0	31.5	5.7

All load-deflection response curves presented in this figure indicate that the deflection variation tends to increase linearly as the load increases before reaching the initial cracking load. The initial stiffness of all samples was close to each other at this stage. At the post-cracking stage, the deflection increased significantly with the application of the load, and the stiffness of all specimens decreased due to flexural cracking. In this stage, slab samples reinforced with steel fibers showed obvious stiffer behavior, and this enhancement increases with increasing fiber content [22]. This enhancement is pronounced in post-cracking flexural stiffness; the sample's structural response is associated with the utilization of steel fiber due to the fibers' ability to withstand tensile strain at cracking surfaces. Finally, after reaching reinforcement yield loading, slab samples showed a dramatic decrease in their flexural stiffness, accompanied by rapidly increasing deflection. This behavior is associated by the nonlinear part of the load-deflection behavior up to failure. Results shown in Figure 11 for the first and second groups indicated that adding EPS beads as a partial replacement of coarse aggregate without steel fiber significantly reduces load carrying capacity and bending resistance when compared with the reference slab sample. On the other hand, results presented in Table 10 and Figure 11 demonstrated the beneficial effect of the added steel fibers on the bending resistance of the tested slabs. The results presented for samples with 20% EPS content showed an increase of about +7.2% and +11.4% in the bending resistance when steel fiber volume fraction was increased to 0.5% and 1%, respectively, whereas for samples with 40% EPS content an increase of about +3.7% and +9.2% was recorded. Regarding the deflection values of the tested slab samples, the results in Table 10 indicated that, in general, as the EPS and steel fiber content increased, the deflection values also increased, suggesting more flexible behavior.

Comparison presented in group three results revealed that increasing EPS beads content from 20% to 40% has little impact on the post-fire bending strength capacity of the tested samples. A reduction of only 3.2% and 2% was noticed when the EPS content doubled for samples with 0.5% and 1% of steel fibers, respectively. This result confirmed the constructive impact of the EPS beads on the structural performance of lightweight slabs exposed to fire or elevated temperature. Hence, Concrete containing lightweight EPS beads is more capable of withstanding high temperatures than conventional aggregate concrete and can maintain its structural integrity for a longer duration under fire exposure. This can also reduce internal stress and prevent spalling during fire exposure. Spalling can lead to a decrease in the strength and stiffness of concrete and expose reinforcing bars to further damage [44, 45].

Comparison of the load-deflection behavior for post-fire samples with those that have not been exposed to fire is presented in Table 11 and Figure 12. Results presented exposed that unburned samples were stiffer than their counterpart subjected to fire, and, generally, burned samples were dramatically weaker. A substantial reduction in the ultimate load and moment capacity was noticed due to fire exposure. Comparison showed that the normal weight reference sample without fiber reinforcement loses 30% of its moment capacity due to fire exposure, whereas a lesser reduction of about 19% to 24% was noted for lightweight EPS samples with different fiber reinforcement proportions. Also, results revealed that burned samples lost only 7.4% and 10.9% of moment capacity compared to 14.9% and 18.6% for unburned samples when 20% and 40% EPS beads were incorporated in the mixture, respectively. This confirmed the positive impact of EPS content in reducing the elevated temperature effect due to its thermal insulation properties. On the other hand, results compiled in Table 11 for unburned samples showed that the flexural strength reduction due to EPS was reduced, whereas a significant improvement in the burned samples' moment capacity was noticed when samples were reinforced with steel fibers. Results depicted an increase of about 15.8% to 20.4% and 16.4% to 22.6% in post-fire ultimate load capacity for the burned samples with 20% and 40% EPS, respectively, due to steel fiber presence.

Table 11. Comparison for burned and unburned samples flexural behaviour

Specimen	Ultimate load (kN)					Max. Deflection (mm)		Variation [1] (%)
	Unburned	Burned	Variation [1] (%)	Variation [2] (%)	Variation [3] (%)	Unburned	Burned	
R	57.6	40.3	-30	----		30.2	26.6	-12
EPS20SF0	49	37.3	-24	-7.4	----	25.6	25.4	-1
EPS20SF0.5	53	43.2	-19		15.8	29.5	27.5	-7
EPS20SF1	58.5	44.9	-23		20.4	30.8	29.8	-3
EPS40SF0	46.9	35.9	-24	-10.9	----	27.4	28.7	5
EPS40SF0.5	53.8	41.8	-22		16.4	30.9	29.6	-4
EPS40SF1	56.5	44	-22		22.6	33.8	31.5	-7

[1] Burned sample results with unburned ones, [2] Burned sample results due to EPS content, [3] Burned sample results due to fiber content.

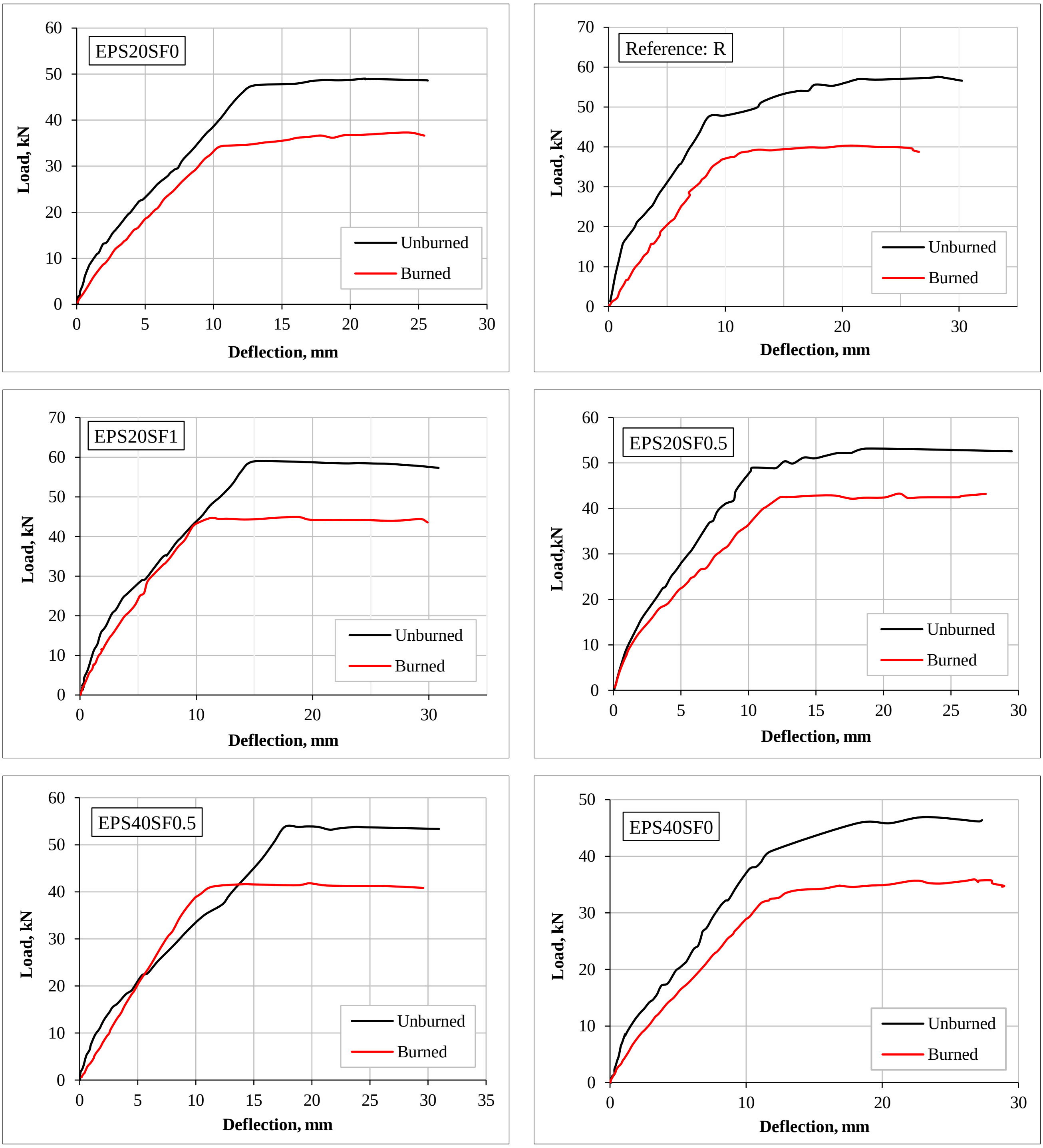

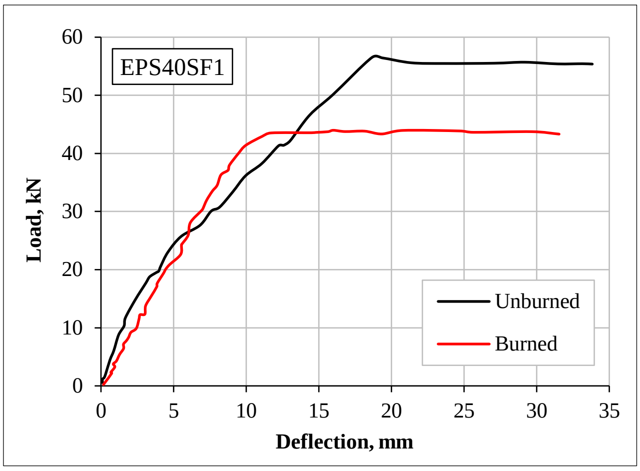

Figure 12. Comparison for load-deflection behaviour for burned and unburned samples

Hence, the greater achievement in the load ultimate load capacity was due to a higher fiber reinforcement volume fraction. This result highlights the beneficial effect of steel fiber reinforcement in strengthening RC lightweight slabs exposed to fire. Regarding the deformability of the post-fire sample, results indicated smaller maximum deflection values compared with unburned samples. This is due to reduced ultimate load capacity for post-fire samples. However, comparing deformability at the same load values revealed greater deflection values for post-fire samples due to reduced stiffness after fire exposure.

3.2.4. Stiffness

Stiffness is the resistance of a deformable body to deflection or distortion due to an applied force. Flexural stiffness is a bending characteristic of a member that can be defined as the resistance of the structure to deflection under bending load [46, 47]. The flexural stiffness is typically characterized by the slope of the line drawn from the origin of the load-deflection curve and the intersection of the curve at the point of interest. The results of the variation in flexural stiffness due to EPS and steel fiber content after fire exposure are listed in Table 12. Results showed that the stiffness of the slab generally decreases when using EPS, while steel fibers enhance stiffness. The decrease in slab stiffness can be primarily attributed to the reduction in the strength of the concrete member due to deterioration resulting from fire exposure. Also, the incorporation of lightweight EPS beads resulted in reduced mechanical properties of the concrete mixture. However, EPS aggregates led to a reduced rate of stiffness deterioration after fire exposure, which is associated with the low thermal conductivity. For samples containing 0% steel fibers, the results showed that a reduction of 9.5% and 21.6% in stiffness values was achieved at 20% and 40% EPS content, respectively. On the other hand, results showed significant enhancement in post-fire flexural stiffness due to fiber reinforcement. An increase in post-fire flexural stiffness of 9.2% and 23.8% was depicted for samples with 20% EPS when reinforced with 0.5% and 1% volume fraction of steel fibers, respectively, whereas this increase was only 9.2% for samples with 40% EPS and 1% steel fiber reinforcement. However, comparison with non-fibrous EPS samples revealed an enhancement up to 36.7% and 39.3% in post-fire flexural stiffness due to 1% fiber reinforcement for samples with 20% and 40% EPS content, respectively.

Table 12. Post-fire stiffness values for the tested slabs

Specimen	P_u	45% (P_u)	Δ @ 45% (P_u)	Stiffness (kN/mm)	Variation [1] (%)	Variation [2] (%)	Variation [3] (%)
R	40.3	18.13	4.40	4.12	----	----	
EPS20SF0	37.3	16.8	4.5	3.73	-9.5	-9.5	----
EPS20SF0.5	43.2	19.44	4.3	4.5	9.2		20.6
EPS20SF1	44.9	20.2	4	5.1	23.8		36.7
EPS40SF0	35.9	16.15	5	3.23	-21.6	-21.6	----
EPS40SF0.5	41.8	18.8	4.6	4.1	-0.5		26.9
EPS40SF1	44	19.8	4.4	4.5	9.2		39.3

[1] Variation with respect to reference, [2] Variation due to EPS content, [3] Variation due to steel fiber content.

3.2.5. Ductility

The ability of a material to withstand deformation over the elastic limit until complete failure is referred to as ductility. The maximum deflection (Δ_{max}) that the materials' can withstand before failing should be considered when assessing ductility. The ductility of two different materials might vary even when they have comparable maximum deflections at failure due to different load-deflection characteristics. So, it is preferable to define the ductility using a dimensionless ductility index, μ, as follows:

$$\mu = \frac{\Delta_{max}}{\Delta_y} \quad (1)$$

The results of the ductility index for the tested samples after fire exposure are presented in Table 13. Ductility index variation illustrates that when EPS was utilized with steel fibers, the ductility increases, whereas introducing only EPS as partial aggregate replacement, i.e., without fibers, mostly causes a reduction in the ductility. Hence, using 20% EPS beads in the concrete mixture leads to a ductility decrease by 13.5%, whereas for 40% EPS beads content, the decrease was only 9.8%. On the other hand, results showed significant enhancement in post-fire ductility due to fiber reinforcement. An increase in post-fire flexural stiffness of 12.8% was depicted for samples with 20% EPS when reinforced with 1% volume fraction of steel fibers, whereas this increase was only 5.3% for samples with 40% EPS. However, comparison with non-fibrous EPS samples revealed an enhancement up to 30.4% and 16.7% in post-fire ductility due to 1% fiber reinforcement for samples with 20% and 40% EPS content, respectively. This result indicated that fiber reinforcement is less effective for samples with higher EPS beads. A lesser ductility enhancement due to steel fiber addition was noted for higher EPS content. One conclusion, based on the above-presented results, is that the addition of a small percentage of EPS and a certain amount of steel fibers largely enhances the material's ductility.

Table 13. Post-fire ductility index values

Specimen	Δ_{max} (mm)	Δ_y (mm)	Ductility index (μ)	Variation[1] (%)	Variation[2] (%)	Variation[3] (%)
R	26.6	10	2.66	----	----	
EPS20SF0	25.4	11	2.3	-13.5	-13.5	----
EPS20SF0.5	27.5	13	2.2	-17.3		-4.3
EPS20SF1	29.8	10	3	12.8		30.4
EPS40SF0	28.7	12	2.4	-9.8	-9.8	----
EPS40SF0.5	29.6	12	2.5	-6		4.2
EPS40SF1	31.5	11	2.8	5.3		16.7

[1] Variation with respect to reference, [2] Variation due to EPS content, [3] Variation due to steel fiber content.

3.2.6. Toughness

Flexural toughness refers to the total capacity of a material to absorb energy. An important property in the field of concrete structures is the ability of a loaded structure to store energy before rupture. The maximum amount of load and deflection seen at the point of failure affects the energy absorbed, which is measured by the area under the load-deflection curve. Hence, the integration of the load-deflection curves of the tested slabs was performed to calculate the flexural toughness, also referred to as the total energy. In this paragraph, an attempt is intended to figure out how elevated temperature affected lightweight EPS slab specimens' toughness.

The total energy of the investigated slabs at the ultimate and failure load is shown in Table 14. The data presented for non-fibrous samples showed that using 20% EPS beads resulted in 14% decrease in the specimens' toughness at failure due to the fire effect, whereas increasing EPS beads to 40% resulted in a decrease of only 6 %. This shows the constructive impact of increasing EPS content due to their thermal characteristics. On the other hand, results showed significant enhancement in post-fire toughness due to fiber reinforcement. An increase in post-fire toughness of 30.5% was depicted for samples with 20% EPS when reinforced with 1% volume fraction of steel fibers, respectively, whereas this increase was 35% for samples with 40% EPS. Furthermore, the same trend for EPS and fiber content effect on post-fire toughness variation is concluded, indicating more enhancement due to steel fiber inclusion. Finally, based on the above results, findings revealed a significant enhancement in the slab toughness when samples reinforced with steel fibers, even though lightweight EPS beads replaced coarse aggregate in the concrete mixture.

Table 14. Post-fire toughness of tested slabs

Specimen	The ultimate load's toughness (kN.mm)	% Toughness variation at ultimate load	The failure load's toughness (kN.mm)	% Toughness variation at failure load		
				(1)	(2)	(3)
R	633.4	-	855.5	-	-	-
EPS20SF0	689.5	9	735.6	-14	-14	-
EPS20SF0.5	684.3	8	957.2	12	-	30.1
EPS20SF1	619.9	-2	1116.8	30.5	-	51.8
EPS40SF0	731.4	15.5	803.3	-6	-6	-
EPS40SF0.5	602.3	-5	1008.2	18	-	25.5
EPS40SF1	476.8	-24.7	1156	35	-	43.9

(1) Variation with respect to reference, (2) Variation due to EPS content, (3) Variation due to steel fiber content.

4. Conclusion

In this study, comprehensive experimental work was performed to investigate the influence of fire exposure on the structural behavior of a lightweight steel fiber-reinforced self-compacting concrete one-way slab. Depending on the study outcomes, several conclusions have been pointed out.

A significant reduction in the mechanical properties of the hardened concrete was observed due to fire exposure. Results indicated that the concrete compressive strength, splitting strength, and modulus of rupture for the reference mixture were reduced by 31.7%, 26%, and 24.4% due to fire exposure, respectively. However, adding EPS beads in the concrete mixture helps in reducing strength degradation due to fire exposure, and the higher the EPS content, the less strength degradation. The flexural strength of the EPS lightweight RC concrete slab without fiber reinforcement, subjected to elevated temperature, was dramatically lower than that of slabs not exposed to fire. However, an obvious increase of 11.4% and 9.2% in the load-carrying capacity was achieved when slab samples containing 20% and 40% of EPS aggregates were reinforced with 1% steel fiber. Moreover, slabs incorporating EPS beads exhibited greater resilience in their ultimate post-burning load capacity. This result revealed the constructive impact of the EPS beads on the structural performance of the RC lightweight slab exposed to fire or elevated temperature due to their low thermal conductivity and insulation properties. Generally, results revealed significant enhancement in post-fire stiffness, ductility, and absorbed energy of the RC slab due to steel fiber inclusion, showing their constructive impact on the performance of the tested RC slab at elevated temperature. Results depicted an increase of about 15.8% to 20.4% and 16.4% to 22.6% in post-fire ultimate load capacity for the burned samples with 20% and 40% EPS, respectively, due to steel fiber presence; hence, the greater achievement in the ultimate load capacity was due to a higher fiber reinforcement volume fraction.

5. Declarations

5.1. Author Contributions

Conceptualization, R.M.A. and A.A.A.; methodology, R.M.A. and A.A.A.; software, A.A.A.; validation, A.A.A.; formal analysis, A.A.A.; investigation, A.A.A.; resources, A.A.A.; data curation, A.A.A.; writing—original draft preparation, A.A.A.; writing—review and editing, R.M.A.; visualization, A.A.A.; supervision, R.M.A.; project administration, R.M.A.; funding acquisition, A.A.A. All authors have read and agreed to the published version of the manuscript.

5.2. Data Availability Statement

The data presented in this study are contained within the article.

5.3. Funding

The authors received no financial support for the research, authorship, and/or publication of this article.

5.4. Conflicts of Interest

The authors declare no conflict of interest.

6. References

[1] Elango, K. S., Sanfeer, J., Gopi, R., Shalini, A., Saravanakumar, R., & Prabhu, L. (2020). Properties of light weight concrete - A state of the art review. Materials Today: Proceedings, 46, 4059–4062. doi:10.1016/j.matpr.2021.02.571.

[2] Chen, B., & Liu, J. (2008). Experimental application of mineral admixtures in lightweight concrete with high strength and workability. Construction and Building Materials, 22(6), 1108–1113. doi:10.1016/j.conbuildmat.2007.03.001.

[3] Kockal, N. U., & Ozturan, T. (2011). Strength and elastic properties of structural lightweight concretes. Materials & Design, 32(4), 2396–2403. doi:10.1016/j.matdes.2010.12.053.

[4] Ünal, O., Uygunoğlu, T., & Yildiz, A. (2007). Investigation of properties of low-strength lightweight concrete for thermal insulation. Building and Environment, 42(2), 584–590. doi:10.1016/j.buildenv.2005.09.024.

[5] Demirboga, R., & Kan, A. (2012). Thermal conductivity and shrinkage properties of modified waste polystyrene aggregate concretes. Construction and Building Materials, 35, 730–734. doi:10.1016/j.conbuildmat.2012.04.105.

[6] Chi, J. M., Huang, R., Yang, C. C., & Chang, J. J. (2003). Effect of aggregate properties on the strength and stiffness of lightweight concrete. Cement and Concrete Composites, 25(2), 197–205. doi:10.1016/S0958-9465(02)00020-3.

[7] Lo, T. Y., Tang, W. C., & Cui, H. Z. (2007). The effects of aggregate properties on lightweight concrete. Building and Environment, 42(8), 3025–3029. doi:10.1016/j.buildenv.2005.06.031.

[8] Carsana, M., Tittarelli, F., & Bertolini, L. (2013). Use of no-fines concrete as a building material: Strength, durability properties and corrosion protection of embedded steel. Cement and Concrete Research, 48, 64–73. doi:10.1016/j.cemconres.2013.02.006.

[9] Anwar Hossain, K. M. (2008). Bond characteristics of plain and deformed bars in lightweight pumice concrete. Construction and Building Materials, 22(7), 1491–1499. doi:10.1016/j.conbuildmat.2007.03.025.

[10] Libre, N. A., Shekarchi, M., Mahoutian, M., & Soroushian, P. (2011). Mechanical properties of hybrid fiber reinforced lightweight aggregate concrete made with natural pumice. Construction and Building Materials, 25(5), 2458–2464. doi:10.1016/j.conbuildmat.2010.11.058.

[11] Gupta, T., Sharma, R. K., & Chaudhary, S. (2015). Impact resistance of concrete containing waste rubber fiber and silica fume. International Journal of Impact Engineering, 83, 76–87. doi:10.1016/j.ijimpeng.2015.05.002.

[12] Maktoof, Y. R., & Abbas, R. M. (2025). Effect of Hybrid Fibers on the Performance of Lightweight Expanded Polystyrene Self-Compacting Concrete. AIP Conference Proceedings, 3303(1), 110014. doi:10.1063/5.0261977.

[13] Ganesh Babu, K., & Saradhi Babu, D. (2004). Performance of fly ash concretes containing lightweight EPS aggregates. Cement and Concrete Composites, 26(6), 605–611. doi:10.1016/s0958-9465(03)00034-9.

[14] Sri Ravindrarajah, R., & Tuck, A. J. (1994). Properties of hardened concrete containing treated expanded polystyrene beads. Cement and Concrete Composites, 16(4), 273–277. doi:10.1016/0958-9465(94)90039-6.

[15] Adeala, A. J., & Soyem, O. B. (2020). Structural Use of Expanded Polystyrene Concrete. International Journal of Innovative Science and Research Technology, 5(6), 1131–1138. doi:10.38124/ijisrt20jun849.

[16] Cook, D. J. (1972). Expanded polystyrene beads as lightweight aggregate for concrete. School of Civil Engineering, University of New South Wales, Kensington, Australia.

[17] Bagon, C., & Frondistou-Yannas, S. (1976). Marine floating concrete made with polystyrene expanded beads. Magazine of Concrete Research, 28(97), 225–229. doi:10.1680/macr.1976.28.97.225.

[18] Prasittisopin, L., Termkhajornkit, P., & Kim, Y. H. (2022). Review of concrete with expanded polystyrene (EPS): Performance and environmental aspects. Journal of Cleaner Production, 366, 132919. doi:10.1016/j.jclepro.2022.132919.

[19] Abbas, R. M., & Fadala, W. A. (2021). Behavioral Investigation of Reinforced Concrete T-Beams with Distributed Reinforcement in the Tension Flange. E3S Web of Conferences, 318, 3010. doi:10.1051/e3sconf/202131803010.

[20] Ali, A., Soomro, Z., Iqbal, S., Bhatti, N., & Abro, A. F. (2018). Comparison of Mechanical Properties of Lightweight and Normal Weight Concretes Reinforced with Steel Fibers. Engineering, Technology & Applied Science Research, 8(2), 2741–2744. doi:10.48084/etasr.1874.

[21] Rakaa, R. K., & Abbas, R. M. (2024). Mechanical Properties of Lightweight EPS Self-compacting Concrete Reinforced with Steel Fibers. Journal of Engineering, 30(06), 125–140. doi:10.31026/j.eng.2024.06.08.

[22] Abbas, R. M., & Rakaa, R. K. (2023). Structural Performance of Lightweight Fiber Reinforced Polystyrene Aggregate Self-Compacted Concrete Beams. Engineering, Technology & Applied Science Research, 13(5), 11865-11870. doi:10.48084/etasr.6217.

[23] Shabbar, R., Al-Tameemi, A. A., & Alhassani, A. M. J. (2022). The effect of expanded polystyrene beads (EPS) on the physical and mechanical properties of aerated concrete. Open Engineering, 12(1), 424–430. doi:10.1515/eng-2022-0020.

[24] Maghfouri, M., Alimohammadi, V., Gupta, R., Saberian, M., Azarsa, P., Hashemi, M., Asadi, I., & Roychand, R. (2022). Drying shrinkage properties of expanded polystyrene (EPS) lightweight aggregate concrete: A review. Case Studies in Construction Materials, 16, 919. doi:10.1016/j.cscm.2022.e00919.

[25] Sun, Y., Li, C., You, J., Bu, C., Yu, L., Yan, Z., Liu, X., Zhang, Y., & Chen, X. (2022). An Investigation of the Properties of Expanded Polystyrene Concrete with Fibers Based on an Orthogonal Experimental Design. Materials, 15(3), 1228. doi:10.3390/ma15031228.

[26] Babu, D. S., Ganesh Babu, K., & Tiong-Huan, W. (2006). Effect of polystyrene aggregate size on strength and moisture migration characteristics of lightweight concrete. Cement and Concrete Composites, 28(6), 520–527. doi:10.1016/j.cemconcomp.2006.02.018.

[27] Vėjelis, S., & Vaitkus, S. (2006). Investigation of water absorbtion by expanded polystyrene slabs. Materials Science (Medžiagotyra), 12(2), 134-137.

[28] Asadi, I., Shafigh, P., Abu Hassan, Z. F. B., & Mahyuddin, N. B. (2018). Thermal conductivity of concrete – A review. Journal of Building Engineering, 20, 81–93. doi:10.1016/j.jobe.2018.07.002.

[29] Mohammed, H. J., & Aayeel, O. K. (2020). Flexural behavior of reinforced concrete beams containing recycled expandable polystyrene particles. Journal of Building Engineering, 32, 101805. doi:10.1016/j.jobe.2020.101805.

[30] Nemes, R., Abed, M. A., Seyam, A. M., & Lublóy, É. (2022). Behavior of structural lightweight concrete produced with expanded clay aggregate and after exposure to high temperatures. Journal of Thermal Analysis and Calorimetry, 147(15), 8111–8118. doi:10.1007/s10973-021-11167-6.

[31] Dabbaghi, F., Nasrollahpour, S., Dehestani, M., & Yousefpour, H. (2022). Optimization of Concrete Mixtures Containing Lightweight Expanded Clay Aggregates Based on Mechanical, Economical, Fire-Resistance, and Environmental Considerations. Journal of Materials in Civil Engineering, 34(2), 4021445. doi:10.1061/(asce)mt.1943-5533.0004083.

[32] Dabbaghi, F., Yang, T. Y., Tanhadoust, A., Emadi, S. B., Dehestani, M., & Yousefpour, H. (2022). Experimental and numerical investigation on post-fire seismic performance of light weight aggregate reinforced concrete beams. Engineering Structures, 268, 114791. doi:10.1016/j.engstruct.2022.114791.

[33] Abdel-Jaber, M., Al-Nsour, R., Shatarat, N., Hasan, H., & Al-zu'bi, H. (2023). Thermal Effect on the Flexural Performance of Lightweight Reinforced Concrete Beams Using Expanded Polystyrene Beads and Pozzolana Aggregate. Engineered Science, 27, 1029. doi:10.30919/es1029.

[34] Dabbaghi, F., Yang, T. Y., Tanhadoust, A., Emadi, S. B., Dehestani, M., & Yousefpour, H. (2022). Experimental and numerical investigation on post-fire seismic performance of light weight aggregate reinforced concrete beams. Engineering Structures, 268, 114791. doi:10.1016/j.engstruct.2022.114791.

[35] Martínez-Martínez, J. E., Álvarez-Rabanal, F. P., Alonso-Martínez, M., & del Coz-Díaz, J. J. (2022). Nonlinear Thermo-Structural Analysis of Lightweight Concrete and Steel Decking Composite Slabs under Fire Conditions: Numerical and Experimental Comparison. Applied Sciences (Switzerland), 12(18), 9306. doi:10.3390/app12189306.

[36] Dabbaghi, F., Dehestani, M., & Yousefpour, H. (2022). Residual mechanical properties of concrete containing lightweight expanded clay aggregate (LECA) after exposure to elevated temperatures. Structural Concrete, 23(4), 2162–2184. doi:10.1002/suco.202000821.

[37] Dabbaghi, F., Nasrollahpour, S., Dehestani, M., & Yousefpour, H. (2022). Optimization of Concrete Mixtures Containing Lightweight Expanded Clay Aggregates Based on Mechanical, Economical, Fire-Resistance, and Environmental Considerations. Journal of Materials in Civil Engineering, 34(2), 4021445. doi:10.1061/(asce)mt.1943-5533.0004083.

[38] Abdullah, A. H., & Mohammed, S. D. (2023). The Fire Effect on the Performance of Reinforced Concrete Beams with Partial Replacement of Coarse Aggregates by Expanded Clay Aggregates. Engineering, Technology & Applied Science Research, 13(6), 12220–12225. doi:10.48084/etasr.6412.

[39] Iraqi Specification No.45. (1984). Aggregate from Natural Sources for Concrete and Construction. Iraqi Organization of Standards, Baghdad, Iraq.

[40] EFNARC. (2005). Specification and Guidelines for Self-Compacting Concrete. European Federation of National Association (EFNARC), Surrey, United Kingdom.

[41] ASTM E119-14. (1992). Standard Test Methods for Fire Tests of Building Construction and Materials. ASTM International, Pennsylvania, United States. doi:10.1520/E0119-14.

[42] Kumar, R., Lakhani, R., & Kumar, A. (2022). Physico-Mechanical and Thermal Properties of Lightweight Structural Concrete with Light Expanded Clay Aggregate for Energy-Efficient Buildings. Advances in Construction Materials and Sustainable Environment. Lecture Notes in Civil Engineering, Vol. 196. Springer, Singapore. doi:10.1007/978-981-16-6557-8_14.

[43] Sayadi, A. A., Tapia, J. V., Neitzert, T. R., & Clifton, G. C. (2016). Effects of expanded polystyrene (EPS) particles on fire resistance, thermal conductivity and compressive strength of foamed concrete. Construction and Building Materials, 112, 716–724. doi:10.1016/j.conbuildmat.2016.02.218.

[44] Song, Y., Fu, C., Liang, S., Li, D., Dang, L., Sun, C., & Kong, W. (2020). Residual Shear Capacity of Reinforced Concrete Beams after Fire Exposure. KSCE Journal of Civil Engineering, 24(11), 3330–3341. doi:10.1007/s12205-020-1758-7.

[45] Zhu, J. M., Wang, X. C., Wei, D., Liu, Y. H., & Xu, B. Y. (2011). Estimation of the residual stiffness of fire-damaged concrete members. Computers, Materials & Continua, 22(3), 261–273.

[46] Mohammad, A. Q., & Abbas, R. M. (2023). Structural Behavior of Prestressed RC Dapped Beam with Openings Strengthened Using CFRP Sheets. E3S Web of Conferences, 427, 2004. doi:10.1051/e3sconf/202342702004.

[47] Sullivan, T. J., Calvi, G. M., & Priestley, M. J. N. (2004, August). Initial stiffness versus secant stiffness in displacement based design. 13th World Conference of Earthquake Engineering (WCEE), 1-6 August, 2004, Vancouver, Canada.